# Study of Deformation Mechanism for Linear Low-Density Polyethylene

MOTONOBU FURUTA, *Takatsuki Research Laboratory, Sumitomo Chemical Co. Ltd., Tsukahara 2-10, Takatsukishi, Osaka, Japan* and SATORU HOSODA and KEITARO KOJIMA, *Chiba Research Laboratory, Sumitomo Chemical Co. Ltd., Anesakikaigan 5-1, Ichiharashi, Chibaken, Japan*

## Synopsis

The deformation mechanism for linear low-density polytheylene (LLDPE) has been studied by electron microscopy, infrared spectroscopy, and pulsed nuclear magnetic resonance. Morphologically, the lamellae in the polar region of a spherulite are aligned in parallel to the drawing direction and then unfolded into microfibrils with drawing. The lamellae in the equatorial region are curved, corrugated, and unfolded partially. Actually, microfibrils are formed with transformation of both lamellae and some amorphous molecules throughout the drawing. Restraint of molecular mobility for the amorphous region increases with drawing, but mobility for the immobile region (lamellae and microfibrils) remains constant. Orientation of the *trans*-methylene sequences in amorphous regions proceeds with extension. These results can explain the changes of the s-s curve behavior.

## INTRODUCTION

It is well known that polyethylene exhibits necking during drawing below the melting temperature, causing the strengthening of the sheets or the films. The drawing behavior has not been well elucidated, probably owing to the insufficient information of the structural changes in polyethylene. Recently, we have studied the deformation mechanism for linear low-density polyethylene (LLDPE) having ethyl branches and reported morphological and polymer chain orientation changes.[1-3] Significant and interesting findings have been obtained with those studies. But, when attention was focused on LLDPE having other than ethyl branches or changes in molecular mobility throughout the drawing process, sufficient information has not yet been obtained.

It was found that spin-spin relaxation time ($T_2$) is associated with the degree of molecular mobility.[4] And studies have been done for natural rubber,[5] *cis*-polybutadien,[6] polypropylene,[7] EPDM,[8] and polyethylene.[9] But, the studies for elongated LLDPE have not been reported. We investigated the deformation mechanism for LLDPE having isobutyl branches by electron microscopy, infrared spectroscopy and $T_2$ measurements to describe the drawing process which accompanies necking at ambient temperature. We have tried to correlate the information provided from each method so as to understand the mechanism.

Journal of Applied Polymer Science, Vol. 33, 401–410 (1987)

CCC 0021-8995/87/020401-10$04.00

## EXPERIMENTAL

**Sample Preparation.** The LLDPE used here was prepared by a low-pressure process using a modified Ziegler-Natta catalyst. The characteristics of this LLDPE were as follows: $d^{20}$ (g/cc); 0.919, isobutyl branch number; 15.4/1000C, Melt Index (in g/10 min for 2.16 kg load at 190°C); 2.1.

For microscopic and $T_2$ measurements, the polymer was moulded into 1 mm thick sheets and then cooled rapidly at ambient temperature. Dumbell-shaped tensile sample sheets (gauge length of 33 mm and width of 6 mm) were stamped out after cooling. Thinner sheets, ca. 200 $\mu$m in thickness, which were prepared by the same procedure as above were used for infrared (IR) study. Sampling was done at each drawing ratio as shown in this paper.

**Stress-Strain Curve.** The stress-strain curve (s-s curve) was measured at room temperature on a tensile tester at a cross-head speed of 10 mm/min.

**Microscopic Observation.** The sheets were sectioned using an ultramicrotome. The specimens for electron microscopic observation were stained by chlorosulfonic and uranic acids. The details for this sample preparation process is described previously.[1] The sectioning of the sheets was done normal to the drawing direction so that the drawing direction in the micrographs could be easily seen from the knife marks in the photos.

**IR Measurement.** Experimental conditions for IR measurements are the same as reported elsewhere.[2]

**$T_2$ Measurement.** Small pieces of drawn and undrawn sheets used for microscopic study were inserted into the nuclear magnetic resonance (NMR) sample tubes. From solid echo sequences, proton $T_2$ was computed by analyzing the FID curves. A Bruker NMR spectrometer, CXP-200 type, was operated at a frequency of 200 MHz for $^1H$ at 30°C. The duration of a 90° pulse and recovering time was 2 $\mu$sec and 7 $\mu$sec, respectively.

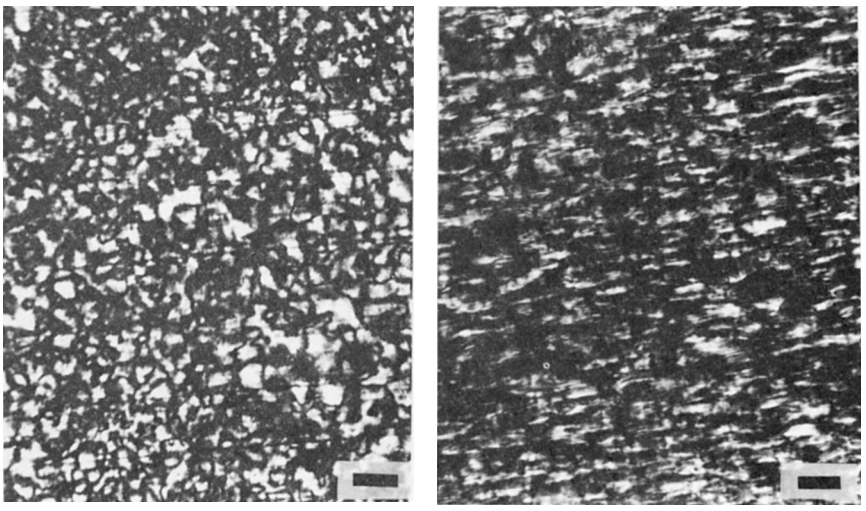

(a) (b)

Fig. 1. Polarized light micrographs of LLDPE: (a) undrawn state; (b) Extension ratio = 3. Drawing direction is vertical in the photo. Scale bar = 20 $\mu$m.

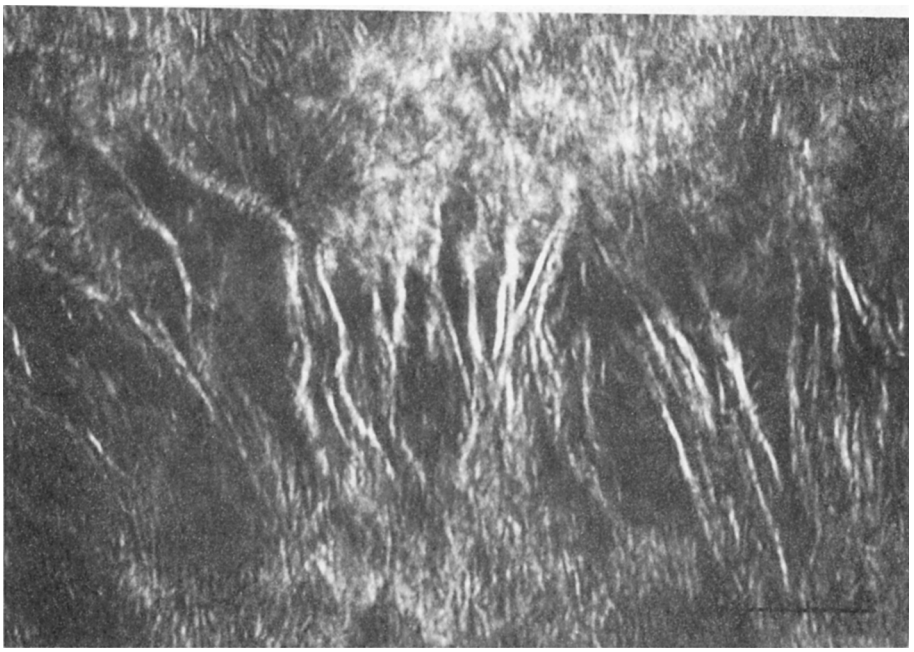

Fig. 2. Electron micrograph of undrawn LLDPE. Scale bar = 0.5 μm.

## RESULTS AND DISCUSSION

In the case of polarization microscopy, the micrographs for undrawn and drawing ratio of 3 of the LLDPE are shown in Figure 1. The spherulites ca. 10 μm in diameter are observed before drawing and they are deformed into ellipsoids at draw ratio of 3. With further drawing, the details of morphology were not seen.

Electron micrographs for the specimens before elongation and draw ratio of 3, 5, and 8 are shown in Figures 2–5, respectively. These micrographs show the typical microstructure features at each drawing stage.

Before drawing, the spherulites are composed of the periodically rotated lamellae as shown in Figure 2 at high magnification. The lamellae ca. 100 Å in width are radial to the center of the spherulite. In Figure 2, the crystalline region gives white contrast and the amorphous region gives dark contrast. With drawing, the morphological changes depend on the region of the spherulite and the drawing direction is defined normal to the equator of the spherulite. In the figures, the elongation direction is indicated by arrows. At a draw ratio of 3, the lamellae in the polar region are aligned in parallel to the drawing direction by the applied stress.

Twisted and curved lamellae in the equatorial region of the spherulite coexist as shown in Figure 3. The tendency for alignment of the lamellae in the polar region in parallel to the elongation direction proceeds at a draw ratio of 5. Figure 4(a) shows the deformation at this drawing stage at low magnification. The bundles of highly aligned lamellae or fibrils ca. 50–100 Å in width in parallel to the elongation direction (region A in the figure) are observed as curved bent lamellae (region B in the figure). At high magnifica-

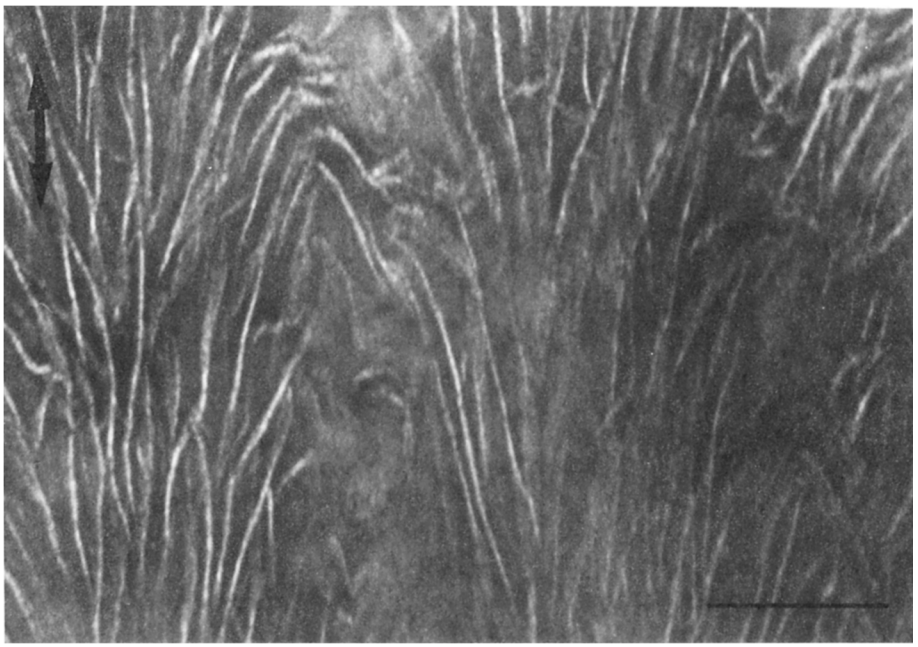

Fig. 3. Electron micrograph of LLDPE for an extension ratio of 3. Arrow indicate drawing direction. Scale bar = 0.5 $\mu$m.

tion [Fig. 4(b)], it is seen that the fibrils ca. 50–80 Å in width exist in region A with the twisted lamellae in region B. It is reasonable to consider that these so-called microfibrils were formed with unfolding of the lamellae by the applied stress, causing the strengthening of the sheet. In other words, transformation of lamella into microfibril brings about necking. At an elongation ratio of 8 (Fig. 5), most of the aligned lamellae are unfolded into microfibrils which are highly aligned in parallel to the elongation direction and form bundles. The microfibrils are also formed from some locations in the corrugated curved lamellae in the equatorial region which appear in the center of the figure. At this drawing stage, the amorphous region adjacent to the microfibrils gives whiter contrast in the figure, indicating that they are highly aligned thus preventing easy penetration of the staining medium. These figures correspond to those for the LLDPE having ethyl branches, supporting the deformation model in our previous work.[1]

Figure 6 is the s-s curve for the LLDPE, showing the typical s-s curve behavior for a crystalline polymer.

In the case of IR study, it is known that the band of 1894 $cm^{-1}$ is due to highly crystalline PE. To obtain the changes in crystallinity for the LLDPE during the drawing process, the absorbance of this purely crystalline band was measured using the unpolarized IR beam.

Figure 7 shows the changes in the crystallinity for the LLDPE during the drawing process using this method. The crystallinity decreases slightly at the start and then increases gradually with further drawing. Differences in crystallinity between the undrawn state and the highly drawn state are very


(a)

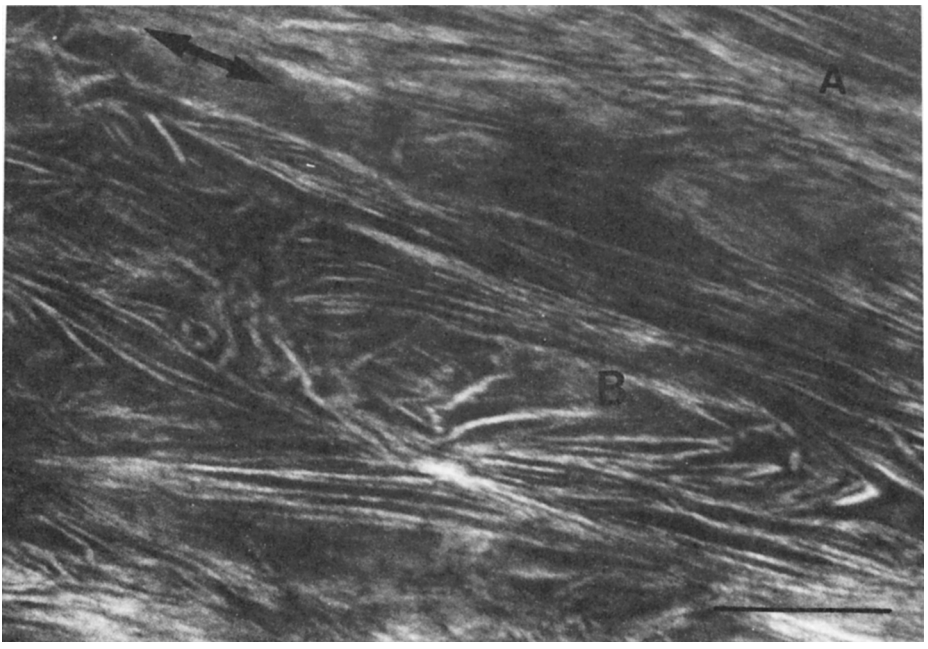


(b)

Fig. 4. Electron micrographs of LLDPE for an extension ratio of 5 at low magnification (a) and high magnification (b). Regions A and B in photos show polar and equatorial regions in spherulite, respectively. Arrows indicate drawing direction. Scale bar is 2 $\mu$m in (a), 0.5 $\mu$m in (b).

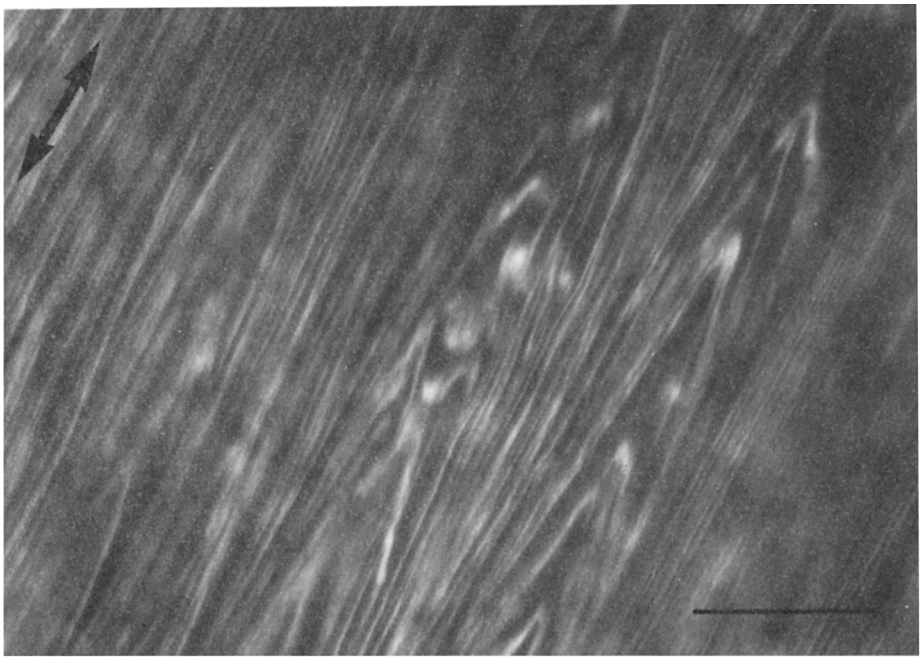

Fig. 5. Electron micrograph of LLDPE for an extension ratio of 8. Arrow indicates the drawing direction. Scale bar = 0.5 $\mu$m.

small, indicating that elongation does not bring about an increase in the crystalline region.

It is reported[10,11] that 2015 $cm^{-1}$ band is a combination of the Raman active fundamental at 1295 $cm^{-1}$ and $CH_2$ rocking bands at 720, 730 $cm^{-1}$. Further this band is based both on crystalline and amorphous phases and is assigned to *trans*-methylene sequences.[12,13] We can therefore estimate the degree of the orientation of the *trans*-methylene sequences in the amorphous

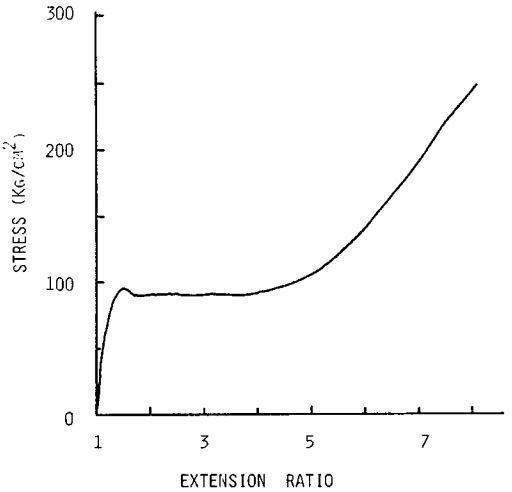


Fig. 6. Stress-strain curve of LLDPE.

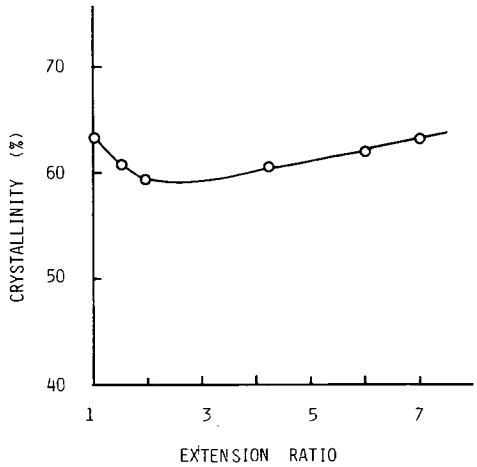


Fig. 7. Changes in crystallinity with extension ratios for LLDPE. (Crystallinity was obtained from IR measurement.)

region by using both 1894 $cm^{-1}$ and 2015 $cm^{-1}$ bands, assuming additivity for orientation and absorbance functions, respectively.

If $f^{cr}$, $f^{am}$, and $f^{tot}$ are the orientation functions of the methylenes in *trans* conformation in the amorphous, crystalline, and total phases, respectively,

$$f^{am} = \left(f^{tot} - \mu_c f^{cr}\right)/(1 - \mu_c) \tag{1}$$

where $\mu_c$ is the fraction of crystalline methylenes in *trans* conformation and is expressed finally as follows:

$$\mu_c = 1/(1 + k_{1894}A_{2015}/k^{am}_{2015}A_{1894} - k^{cr}_{2015}/k^{am}_{2015}) \tag{2}$$

Here, $k_{1894}$ is the absorptivity of 1894 $cm^{-1}$ band, and $k^{cr}_{2015}$, $k^{am}_{2015}$ are the absorptivities for the crystalline and the amorphous parts of the 2015 $cm^{-1}$ band, respectively.

The orientation function of the methylene sequences in *trans* conformation throughout the extension process is shown in Figure 8. $f^{am}$ increases with increasing extension ratio, depicting a trace similar to the s-s curve for this sample, and it shows a fairly high degree of orientation.

These facts are probably due to the higher rigidity of the *trans*-methylene sequences in the amorphous phase, which is supposed to be intimately related to the tie chains suggested by Glenz and Peterlin.[14-16]

Next we will describe the results for studying the molecular mobility during the drawing process using pulsed NMR. Figure 9 shows the free induction decays (FID) at each extension stage. The FID curves were well fitted by the sum of two components as follows within the limits of experimental errors, so

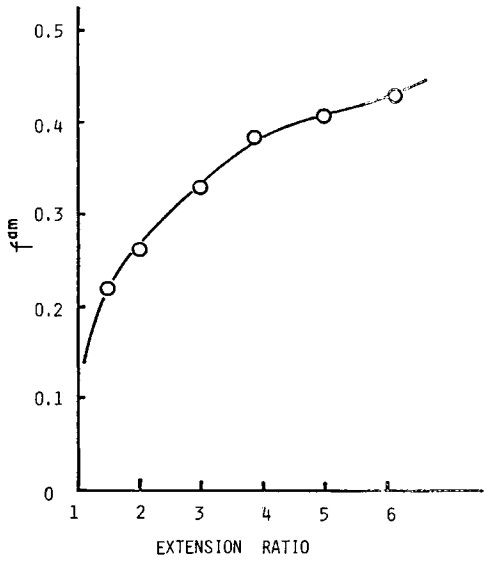


Fig. 8. Relative reduced orientation function vs. extension ratio for *trans*-methylene sequences in amorphous phase of LLDPE.

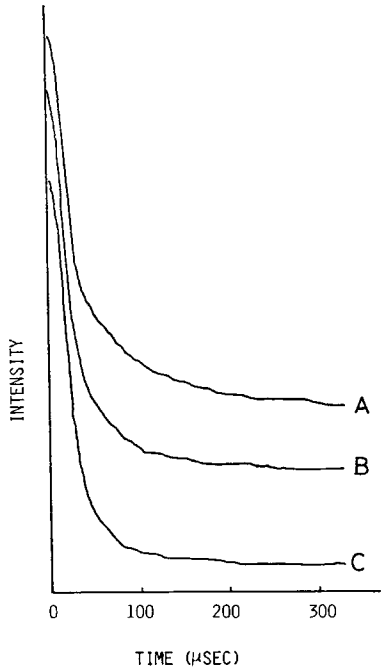


Fig. 9. Spin-spin relaxation decays for LLDPE; A: undrawn, B: extension ratio = 3, C: extension ratio = 6.5.

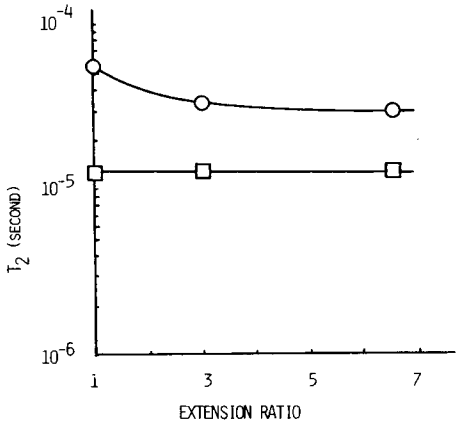


Fig. 10. Variations of $T_2$ for LLDPE with extension ratios; ○: amorphous phase, □: restrained molecular phase.

we can see the changes of molecular mobility for each component throughout the extension process.

$$A \exp(-t/T_{2L}) + B \exp(-t/T_{2S})^2 \tag{3}$$

Here, $t$ is the time, $A + B = 1$, and shorter $T_2$ is expressed as $T_{2S}$, and longer one is $T_{2L}$. Figure 10 shows the changes of each $T_2$ during the drawing process. $T_{2S}$ remains constant with drawing, on the contrary, $T_{2L}$ decreases slightly with drawing. Since $T_{2S}$, contributing to both lamella and microfibril, remains constant, there is little difference between restriction of chain mobility by lamella and microfibril. The initial decrease of $T_{2L}$ indicates, according to the authors, the increased restriction of molecular mobility in the amorphous phase of the polyethylene. The fraction of the chain sections contributing to $T_{2S}$ increases with draw ratio (from 1 to 7) from 59 to 72% as shown in Figure 11. The fraction before drawing (about 59%) is comparable to the crystallinity (62%) from IR measurement but the crystallinity does not increase considerably with the draw ratios (Fig. 7). The results can be explained as the steady increase of the highly restrained molecules ($T_{2S}$ component) is much more than the crystallinity increase. So, it is reasonable to consider that increase in the highly restrained portion is due to the increased microfibrils formed with unfolding of the lamellae. It can be explained as follows; when unfolding of the lamellae occurs, some portion of the molecules in the amorphous phase are transformed into the microfibrils with the molecules in the crystalline region, which results in an increase in the volume of $T_{2S}$ component throughout the drawing process. It is very interesting the highly restrained component which was not seen as the crystalline region from IR measurements was determined quantitatively in the drawn LLDPE from $T_2$ measurements. Slight differences in molecular mobility between lamella and microfibril throughout the drawing process might suggest that lamella or microfibril is the highest restrained state for polyethylene.

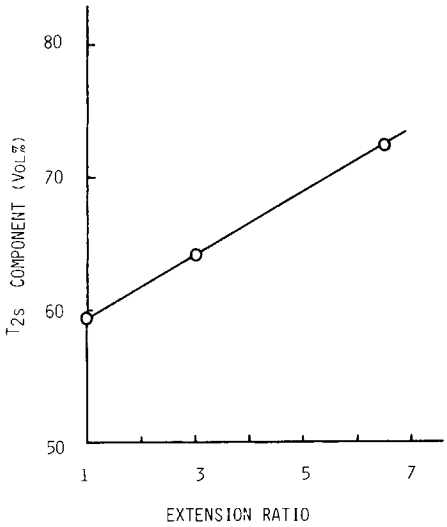


Fig. 11. Change of $T_{2S}$ component fraction with extension ratios.

These changes in molecular mobility are correlated with the orientation of the *trans*-methylene sequences in the amorphous phase which describe the s-s curve behavior.

## References

1. M. Furuta and K. Kojima, *J. Macromol. Sci., Phys.*, **B25**, 349 (1986).
2. S. Hosoda and M. Furuta, *Makromol. Chem. Rapid Commun.*, **2**, 577 (1981).
3. S. Hosoda, *Makromol Chem.*, **185**, 787 (1984).
4. R. Kubo and K. Tomita, *J. Polym. Soc. Japan.*, **9**, 881 (1954).
5. T. Nishi, *J. Polym. Sci. Phys.*, **12**, 685 (1974).
6. J. O'Brien, E. Cashell, G. E. Wardell, and V. J. Mcbriery, *Macromolecules*, **9**, 653 (1976).
7. M. Ito, H. Serizawa, K. Tanaka, W. P. Leung, and C. L. Choy, *J. Polym. Sci., Phys.*, **21**, 2299 (1983).
8. M. Furuta, T. Hikasa, and E. Kato, *J. Appl. Polym. Sci.*, **31**, 2325 (1986).
9. I. Kamel, and A. Charlesby, *J. Polym. Sci., Phys.*, **19**, 803 (1981).
10. J. R. Nielsen and R. F. Holland, *J. Mol. Spectrosc.*, **6**, 394 (1961).
11. J. R. Nielsen and A. H. Woolett, *J. Chem. Phys.*, **26**, 1391 (1957).
12. B. E. Read and R. S. Stein, *Macromolecules*, **1**, 116 (1968).
13. B. E. Read and D. A. Hughes, *Polymer.*, **13**, 495 (1972).
14. W. Glenz and A. Peterlin, *J. Polym. Sci., A*-2., **9**, 1191 (1971).
15. A. Peterlin, *J. Polym. Sci., A*-2., **7**, 1151 (1969).
16. A. Peterlin, *J. Mater. Sci.*, **6**, 490 (1971).

Received April 8, 1986
Accepted June 27, 1986